THE AMERICAN SOCIETY OF MECHANICAL ENGINEERS
345 E. 47 St., New York, N.Y. 10017

91-JPGC-NE-27

Transient Response of Large Inertia Cross Flow Heat Exchangers

K.P. Singh, Ph.D., PE
President and CEO
Holtec International

and

Yu Wang
and
K. Iulianetti

INTRODUCTION

The "cross-flow" heat exchanger is a generic term to describe heat exchange equipment wherein the in-tube fluid flows at right angles to the shell side fluid[1]. Cross-flow exchangers are commonly used when the fluid medium on the shell side is gaseous, resulting in large volumetric flow rates. Arranging the shell side stream to flow orthogonally to the tube bundle provides the largest possible cross-sectional flow area for the shell side fluid to best accommodate the large volume of flow. This simple imperative of design underlies the nearly universal cross-flow arrangement employed in a wide variety of tubular exchangers such as air coolers and flue gas recuperators. Low film coefficients associated with convective heat transfer of gases mean that the heat exchanger would be relatively bulky for moderate heat duty requirements. Some cross-flow exchangers can indeed become quite massive; the flue gas recuperator for Alabama Electric Cooperative's Compressed Air Energy Storage (CAES) plant, at 1.7 million pounds, is a case in point. Fabricated and installed in late 1990 as the world's first recuperator equipped compressed air energy plant, this exchanger extracts heat from flue gas at 696°F nominal temperature to preheat the cavern air from 95°F to 546.6°F delivering a total heat duty of 138 million Btu/hr. A comparable water-to-water heat exchanger, i.e., one required to meet identical heat load at identical end point temperatures, would weigh approximately 150 thousand lbs. In other words, the gaseous exchanger is roughly 11 times as massive as a liquid unit!

In many instances, it is necessary to predict the transient response of cross-flow exchangers to variations in the input quantities, namely flow rates and inlet temperatures. For example, the time varying temperature of air supplied to the furnace burner in a preheating recuperator during the startup period is an important operational concern.

The great bulk and large thermal capacitance of the cross-flow exchangers is not a matter of much heat transfer concern during steady state conditions. However, transient conditions are another matter. Whereas the tube bundle in a liquid-to-liquid exchanger follows the temperature profiles of the shell side and tube side fluids with a very short lag, the response of the cross-flow bundle is considerably sluggish.

The "sluggish" response problem motivated us to develop a methodology to analyze the unsteady state response of outlet temperatures to a ramp variation of input quantities of cross flow recuperators. The approach is general and can be applied to any cross flow shell-and-tube heat exchangers with large thermal inertia.

The concept of the approach is to break the equipment into a number of individual heat transfer units. Similar to finite element methods, a global governing equation is obtained through systematic matrix analysis. The governing equation is a set of differential equations which can be easily solved numerically. In this paper, detail mathematical deviations are provided. An illustrative example is given. The numerical difficulties in solving the specific differential equations are also described.

NOMENCLATURE

A = Overall heat transfer area of tubes

Presented at the International Power Generation Conference
October 6-10, 1991—San Diego, CA

A_i = Heat transfer area of tubes in heat transfer unit i
A_{si} = Heat transfer area of shell in unit i
C_p = Heat capacity
h_{fi} = Film coefficient at outside tube wall surface in unit i
h_{ai} = Film coefficient at inside tube wall surface in unit i
h_{si} = Film coefficient at inside shell wall surface in unit i
H_i = Thermal inertia in heat transfer unit i
ℓ = Element length in y, the tube side flow direction
L = Element length in x, the shell side flow direction
m = Thermal flow rate
r = Tube radius
t_j = Tube side fluid temperature between component j and (j+1)
t_{Aj} = Tube side fluid averag temperature in fluid component j
T_i = Shell side fluid temperature between component i and (i+1)
T_{Ai} = Shell side fluid average temperature in component i
u = Mass flow rate of fluid
V_i = Control volume in heat transfer unit i
θ_i = Shell metal average temperature in heat transfer unit i
ϕ_i = Tube metal average temperature in heat transfer unit i
τ = Time coordinate
ρ = Density

Subscript

f = Shell side fluid
a = Tube side fluid
s = Shell metal
t = Tube metal

Superscript

i = Heat transfer unit and shell side fluid component designator
j = Tube side fluid component designator

ANALYSIS

Cross-Flow Heat Exchangers

In a shell-and-tube heat exchanger, two flows, namely the tube side flow and shell side flow, are separated from each other by the tube walls. Heat is conducted through the tube walls. In a cross flow shell-and-tube heat exchanger, as shown in Figure 1, the tubes are perpendicular to the shell side flow. A heat exchanger may have any number of shell or tube passes. In the following, we assume single shell pass. That is, the shell side flow goes directly through the heat exchanger from one end to the other. We also assume that the heat exchanger has N tube passes. The arrangement of tube passes has significant effects on the overall heat transfer performance of a cross flow shell-and-tube heat exchanger.

A cross flow shell-and-tube heat exchanger can be discretized into N he transfer units. A heat transfer unit contai four types of discretized thermal inertia: a unit of shell metal, a control volume of shell side flow, volume of tube metal in the unit, and a control volume of tube side flow. When we discretized the equipment into heat transfer units, we have also discretized the shell and tube metal, and the shell and tube side fluids. Here we setup a numbering system for our mathematical modeling and computer programming. In our numbering system, we assume that in heat transfer unit i tube side fluid component j is in contact with the shell side fluid component i. The shell side flow unit designator is consistent with the heat transfer unit designator. That is, the heat transfer units are generated in a way that the first unit starts from the shell side flow inlet and the rest of the units are arranged in sequence along the shell side flow. The last unit is located at the outlet of the shell side flow. The tube side flow units are also generated in sequence from the inlet to the outlet of the tube side flow. The heat transfer numbering system is shown in Figure 2.

Assumptions

The following assumptions have been used in our formulations:

1) Radial temperature gradient across e metal or fluid is negligible;
2) Constant heat transfer film coefficients;
3) The equipment is insulated. That is, there is no heat loss to the surroundings.

One Dimensional Flow Transient

Consider a one-dimensional flow with uniform velocity moving in the x direction in a circular tube of radius r as shown in Figure 3. Surface convective heat transfer takes place between the fluid and the wall with a film heat transfer coefficient of h_c. The tube wall temperature is T_w. Taking the energy balance over an infinitely small control volume of length dx, we can derive

$$dx\,\rho\,r^2\pi\,C_p\frac{\partial T}{\partial \tau} = -r^2\pi\frac{\partial}{\partial x}\left(k\frac{\partial T}{\partial x}\right)dx - u\,C_p\frac{\partial T}{\partial x}dx - 2h_c r\,\pi\,dx(T-T_w) \quad (1)$$

or

$$H\frac{\partial T}{\partial \tau} = -P\frac{\partial^2 T}{\partial x^2} - m\frac{\partial T}{\partial x} - U(T-T_w) \quad (2)$$

where $H=\rho r^2\pi C_p$; $P=r^2\pi k$; $m=uC_p$; $U=2h_c r\pi$.

If we discretize the continuous flow into a network or mesh of points and the temperatures unknown are sought only at those discrete points rather than everywhere in the domain, a numerical solution can be found. I us equally space the flow in x. If t constant difference between successive values of x is L, so that x can be expressed as

$=x_o + rL \qquad r= \ldots -2,-1,0,1,2,\ldots \qquad (3)$

a corresponding temperature function is

$$T_r= f(x_o + rL) \qquad (4)$$

We use T_A as the average temperature between node i and (i-1), and

$$\frac{\partial T_A}{\partial x} = \frac{T_i-T_{i-1}}{L} \qquad (5)$$

We also assume that any conduction heat transfer is negligible, then Eqn.(2) becomes

$$H\frac{\partial T_A}{\partial \tau} = m(T_{i-1}-T_i) - U(T_A-T_{wi}) \qquad (6)$$

where $H=\rho r^2\pi C_p h$; $m=uC_p$; $U=2h_c r\pi h$. To be general, $H=V\rho C_p$; $U=A_p h_c$. V is the discretized control volume. A_p is the total heat transfer surface area of V with respect to h_c. Eqn.(6) is the governing heat balance equation of the following numerical analysis.

Formulations for Heat Transfer Units

Now consider the heat transfer unit we have described. A typical heat transfer unit i is shown in Figure 4. The unit i contains shell side fluid component i and tube side fluid component j. We assume that the steady state is disturbed by changing the inlet temperatures or flow rates. Based on the above assumptions, four heat balance equations like Eqn. (6) for the shell side fluid, the tube side fluid, the tube metal, and shell metal are generated:

$$\left.\begin{aligned} H_{fi}\frac{dT_{Ai}}{d\tau} &= m_f(T_{i-1}-T_i) - h_{fi}A_i(T_{Ai}-\phi_i) - h_{si}A_i(T_{Ai}-\theta_i) \\ H_{ti}\frac{d\phi_i}{d\tau} &= h_{fi}A_i(T_{Ai}-\phi_i) - h_{ai}A_i(\phi_i-t_{Aj}) \\ H_{ai}\frac{dt_{Aj}}{d\tau} &= m_a(t_{j-1}-t_j) + h_{ai}A_i(\phi_i-t_{Aj}) \\ H_{si}\frac{d\theta_i}{d\tau} &= h_{si}A_{si}(T_{Ai}-\theta_i) \end{aligned}\right\} \qquad (7)$$

The thermal inertia of the fluid on each side and both the tube and the shell metals can be defined as:

$$\left.\begin{aligned} H_{fi} &= C_{pf}\rho_f V_{fi} \\ H_{ti} &= C_{pt}\rho_t V_{ti} \\ H_{ai} &= C_{pa}\rho_a V_{ai} \\ H_{si} &= C_{ps}\rho_s V_{si} \end{aligned}\right\} \qquad (8)$$

Let

$$\{y^i\}=\begin{Bmatrix} T_{Ai} \\ \phi_i \\ t_{Aj} \\ \theta_i \end{Bmatrix} \qquad \{d^i\}=\begin{Bmatrix} T_i \\ 0 \\ t_j \\ 0 \end{Bmatrix} \qquad (9)$$

Then Eqn. (7) can be expressed in the following matrix form:

$$\{\dot{y}^i\}=[Q^i]\,[\{d^i\}-\{d^{i-1}\}]+[F^i]\{y^i\} \qquad (10)$$

where

$$[F^i]=\begin{bmatrix} -\frac{U_{fi}A_i+h_{si}A_{si}}{H_{fi}} & \frac{h_{fi}A_i}{H_{fi}} & 0 & \frac{h_{si}A_{si}}{H_{fi}} \\ \frac{h_{fi}A_i}{H_{ti}} & -\frac{h_{fi}A_i+U_{ai}Ai}{H_{ti}} & \frac{h_{ai}A_i}{H_{ti}} & 0 \\ 0 & \frac{h_{ai}A_i}{H_{ai}} & -\frac{h_{ai}A_i}{H_{ai}} & 0 \\ \frac{h_{si}A_{si}}{H_{si}} & 0 & 0 & -\frac{h_{si}A_{si}}{H_{si}} \end{bmatrix} \qquad (11)$$

and

$$[Q^i]=\begin{bmatrix} \frac{m_f}{H_{fi}} & 0 & 0 & 0 \\ 0 & 0 & 0 & 0 \\ 0 & 0 & \frac{m_a}{H_{fi}} & 0 \\ 0 & 0 & 0 & 0 \end{bmatrix} \qquad (12)$$

Let

$$\{\zeta^i\}=\begin{Bmatrix} T_{i-1} \\ T_i \end{Bmatrix} \qquad \{\eta^i\}=\begin{Bmatrix} t_{j-1} \\ t_j \end{Bmatrix} \qquad (13)$$

We now need to represent the average temperature within a unit in terms of the nodal temperature at the either end of the unit. The temperature distribution in each fluid stream along the flow direction in the unit can be expressed as:

$$\left.\begin{aligned} T &= [N_{ix}]\{\zeta^i\} \\ t &= [N_{iy}]\{\eta^i\} \end{aligned}\right\} \qquad (14)$$

N_{ix}, N_{iy} are shape functions in terms of a local coordinate, within a unit, in the direction of flow. The average fluid temperature in the unit can be integrated as:

$$\left.\begin{aligned} T_{Ai} &= \frac{1}{L}\int_0^L T\,dx = [B_x^i]\{\zeta^i\} \\ t_{Aj} &= \frac{1}{\iota}\int_0^\iota t\,dy = [B_y^i]\{\eta^i\} \end{aligned}\right\} \qquad (15)$$

that is,

$$\begin{Bmatrix} T_{Ai} \\ t_{Aj} \end{Bmatrix}=\begin{bmatrix} B_{1x}^i & 0 \\ 0 & B_{1y}^i \end{bmatrix}\begin{Bmatrix} T_{i-1} \\ t_{j-1} \end{Bmatrix}+\begin{bmatrix} B_{2x}^i & 0 \\ 0 & B_{2y}^i \end{bmatrix}\begin{Bmatrix} T_i \\ t_j \end{Bmatrix} \qquad (16)$$

Depending on the shape function chosen, Eqn.(16) gives the relation of T_{Ai}, t_{Aj} in terms of T_{i-1}, T_i, t_{j-1}, and t_j. Substitute (16) into Eqn. (10), we have

$$\{\dot{y}^i\} = [R^i]\{d^{i-1}\} + [K^i]\{y^i\} \quad (17)$$

where

$$[K^i] = \begin{bmatrix} -Q_{11}^i B_{2x}^{i-1} + F_{11}^i & F_{12}^i & F_{13}^i & F_{14}^i \\ F_{21}^i & F_{22}i & F_{23}^i & F_{24}^i \\ F_{31}^i & F_{32}^i & -Q_{33}^i B_2 y^{-1} + F_{33}^i & F_{34}^i \\ F_{41}^i & F_{42}^i & F_{43}^i & F_{44}^i \end{bmatrix} \quad (18)$$

and

$$[R^i] = \begin{bmatrix} (1+(B_{2x}^i)^{-1}B_{1x}^i)\,Q_{11}^i & 0 & 0 & 0 \\ 0 & 0 & 0 & 0 \\ 0 & 0 & (1+(B_{2y}^i)^{-1}B_{1y}^i)\,Q_{33}^i & 0 \\ 0 & 0 & 0 & 0 \end{bmatrix} \quad (19)$$

As we noted, there are total of N heat transfer units in the equipment. Therefore, the global governing equation can be expressed as:

$$\{\dot{y}\} = \sum_{i=1}^{N} \left([R^i]\{d^{i-1}\} + [K^i]\{y^i\} \right) \quad (20)$$

Substitute (16) into (20), we have

$$\{\dot{y}\} = \{d^o\} + [K]\{y\} \quad (21)$$

where

{d°} = boundary condition matrix;
[K] = global transient efficient matrix.
These equations are sufficient to solve

for the nodal temperatures in each stream once appropriate loading conditions are set.

Instability

Because of the flow term, numerical instability may occur[2-4]. Upwinding is suggested to eliminate the instability problem[2-4]. For certain flow values, use of linear shape functions will cause instability even if we have very fine meshes[2]. In the following, we show that a modified non-linear shape function can be used as an alternate to upwinding.

We also noted that Eqn. (21) are transient differential equations, the temperature shapes are also time dependent. A sharp gradient occurs if the transient condition comes from a step ramp in inlet temperature. In such cases, the first order transient differential equations (21) may become stiff. The stiff problem is also discussed.

Shape Function

Linear Shape Function:

$$\left.\begin{aligned} N_{1x} &= 1 - \frac{x}{L} \\ N_{2x} &= \frac{x}{L} \end{aligned}\right\} \quad (22)$$

From Eqn. (15),

$$\left[B_x^i\right] = \left[\frac{1}{2} \quad \frac{1}{2}\right] \quad (23)$$

Then, Eqn. (16) becomes

$$\begin{Bmatrix} T_{Ai} \\ t_{Aj} \end{Bmatrix} = \begin{bmatrix} \frac{1}{2} & 0 \\ 0 & \frac{1}{2} \end{bmatrix} \begin{Bmatrix} T_{i-1} \\ t_{j-1} \end{Bmatrix} + \begin{bmatrix} \frac{1}{2} & 0 \\ 0 & \frac{1}{2} \end{bmatrix} \begin{Bmatrix} T_i \\ t_j \end{Bmatrix} \quad (24)$$

For many problems, use of Eqn.(24) will not provide correct results.

Modified Non-Linear Shape Function:

$$\left.\begin{aligned} N_1(x) &= 1 - 3\frac{x^2}{L^2} + 2\frac{x^3}{L^3} \\ N_2(x) &= x - 2\frac{x^2}{L} + \frac{x^3}{L^2} \\ N_3(x) &= 3\frac{x^2}{L^2} - 2\frac{x^3}{L^3} \\ N_4(x) &= -\frac{x^2}{L} + \frac{x^3}{L^2} \end{aligned}\right\} \quad (25)$$

We define

$$\{\psi^i\} = \begin{Bmatrix} t_{i-1} \\ \frac{dT_{i-1}}{dx} \\ T_i \\ \frac{dT_i}{dx} \end{Bmatrix} \quad (26)$$

then

$$T_i = \left[N_x^i\right]\{\psi^i\} \quad (27)$$

where

$$\left.\begin{aligned} \frac{dT_{i-1}}{dx} &= f_1^i(\tau) \\ \frac{dT_i}{dx} &= f_2^i(\tau) \end{aligned}\right\} \quad (28)$$

When time coordinate τ varies from 0 to ∞, $f_1^i(\tau)$ changes from $-\infty$ to $(T_1 - T_2)/L$; and $f_2^i(\tau)$ changes from 0 to $(T_1 - T_2)/L$. We assume that the gradient functions have the following form:

$$f_1^i(\tau)=\frac{T_{i-1}-T_i}{L}(-Ae^{-\lambda\tau}-1)$$
$$f_2^i(\tau)=\frac{T_{i-1}-T_i}{L}(e^{-\lambda\tau}-1) \qquad (29)$$

where A and λ are constants and will be discussed later. From Eqn.(15), we have

$$\left[B_x^i\right] = \left[\frac{1}{2}\ \frac{L}{12}\ \frac{1}{2}\ -\frac{L}{12}\right] \qquad (30)$$

The average temperature becomes

$$T_{Ai}=\frac{L}{12}[f_1^i(\tau)-f_2^i(\tau)]+\frac{1}{2}(T_{i-1}+T_i)$$
$$=-\frac{(A+1)e^{-\lambda\tau}}{12}(T_{i-1}-T_i)+\frac{1}{2}(T_{i-1}+T_i) \qquad (31)$$

If we assume that only the shell side flow has ramp inlet, and the temperature gradient is assumed non-linear, and the tube side flow temperature gradient in the unit is assumed linear, then we have

$$\begin{Bmatrix}T_{Ai}\\ t_{Aj}\end{Bmatrix}=\begin{bmatrix}(\frac{1}{2}-\frac{(A+1)e^{-\lambda\tau}}{12}) & 0\\ 0 & \frac{1}{2}\end{bmatrix}\begin{Bmatrix}T_{i-1}\\ t_{j-1}\end{Bmatrix}+\begin{bmatrix}(\frac{1}{2}+\frac{(A+1)e^{-\lambda\tau}}{12}) & 0\\ 0 & \frac{1}{2}\end{bmatrix}\begin{Bmatrix}T_i\\ t_j\end{Bmatrix} \qquad (32)$$

Constant A. -(A+1) is the initial temperature slope with respect to length coordinate x. We may assume

$$A+1=\frac{T_1}{L/2}$$
$$A=\frac{2T_1}{L}-1 \qquad (33)$$

Constant λ. λ controls the convergence speed from non-linear shape to linear shape. λ is always greater than 0. The higher the value of λ, the faster the shape is converged to a linear form. A reasonable value of λ should be assumed based upon to the problem.

Stiffness

When the Jacobian matrix of an ordinary differential equation system has an eigenvalue whose real part is large in magnitude compared to the reciprocal of the time span of interest, stiffness occurs. In our problem, if the input has a ramp, the governing differential equation system may become stiff. In this case, solvers with the capability to resolve the stiffness are required.

ILLUSTRATIVE EXAMPLE

Figure 5 shows the described CAES plant flue gas preheating recuperator. Flue gas from the furnace is on the shell side. Cold air is heated in the tube side and is then supplied to the furnace. The objective is to analyze the initial response of the equipment during the start up of the operation. There are sixteen tube passes which can be divided into three sections(see Figure 5). Each section represents a continuous segment of air in contacting with a continuous segment of flue gas with continuous temperature gradient. For the illustration, we use a three unit problem. The three heat transfer units represent different sections and are designated sequentially from flue gas inlet to outlet. The sketch of the model is shown in Figure 6. Since the flue gas inlet temperature has been assumed as an initial step ramp in time, we use non-linear shape function for the flue gas temperature gradient in the first unit. All other shape functions are assumed linear. The detailed formulation is shown below:

For Unit 1:

$$\begin{Bmatrix}T_{A1}\\ t_{A3}\end{Bmatrix}=\begin{bmatrix}\frac{1}{2}-\frac{(A+1)e^{-\lambda\tau}}{12} & 0\\ 0 & \frac{1}{2}\end{bmatrix}\begin{Bmatrix}T_o\\ t_2\end{Bmatrix}+\begin{bmatrix}\frac{1}{2}+\frac{(A+1)e-\lambda\tau}{12} & 0\\ 0 & \frac{1}{2}\end{bmatrix}\begin{Bmatrix}T_1\\ t_3\end{Bmatrix} \qquad (34)$$

Let

$$A_1=\frac{1}{2}-\frac{(A+1)e^{-\lambda\tau}}{12}$$
$$A_2=\frac{1}{2}+\frac{(A+1)e^{-\lambda\tau}}{12} \qquad (35)$$

then

$$T_1=-\frac{A_1}{A_2}T_o+\frac{1}{A_2}T_{A1}$$
$$t_3=-t_2+2t_{A3} \qquad (36)$$

then Eqn. (17) becomes

$$\begin{pmatrix}\dot{T}_{A1}\\ \dot{\phi}_1\\ \dot{t}_{A3}\\ \dot{\theta}_1\end{pmatrix}=\begin{pmatrix}(1+\frac{A_1}{A_2})Q_{11}^1T_o\\ 0\\ 2Q_{33}^1t_2\\ 0\end{pmatrix}+\begin{bmatrix}-\frac{Q_{11}^1}{A_2}+F_{11}^1 & F_{12}^1 & F_{13}^1 & F_{14}^1\\ F_{21}^1 & F_{22}^1 & F_{23}^1 & F_{24}^1\\ F_{31}^1 & F_{32}^1 & -2Q_{33}^1+F_{33}^1 & F_{34}^1\\ F_{41}^1 & F_{42}^1 & F_{43}^1 & F_{44}^1\end{bmatrix}\begin{bmatrix}T_{A1}\\ \phi_1\\ t_{A3}\\ \theta_1\end{bmatrix} \qquad (37)$$

For Unit 2 and 3:

$$\begin{Bmatrix}T_{Ai}\\ t_{Aj}\end{Bmatrix}=\begin{bmatrix}\frac{1}{2} & 0\\ 0 & \frac{1}{2}\end{bmatrix}\begin{Bmatrix}T_{i-1}\\ t_{j-1}\end{Bmatrix}+\begin{bmatrix}\frac{1}{2} & 0\\ 0 & \frac{1}{2}\end{bmatrix}\begin{Bmatrix}T_i\\ t_j\end{Bmatrix} \qquad (38)$$

Eqn.(17) becomes:

$$\begin{pmatrix} \dot{T}_{A2} \\ \dot{\varphi}_2 \\ \dot{t}_{A1} \\ \dot{\theta}_2 \end{pmatrix} = \begin{pmatrix} 2Q_{11}^2 T_o \\ 0 \\ 2Q_{33}^2 t_2 \\ 0 \end{pmatrix} + \begin{bmatrix} -2Q_{11}^2+F_{11}^2 & F_{12}^2 & F_{13}^2 & F_{14}^2 \\ F_{21}^2 & F_{22}^2 & F_{23}^2 & F_{24}^2 \\ F_{31}^2 & F_{32}^2 & -2Q_{33}^2+F_{33}^2 & F_{34}^2 \\ F_{41}^2 & F_{42}^2 & F_{43}^2 & F_{44}^2 \end{bmatrix} \begin{bmatrix} T_{A2} \\ \varphi_2 \\ t_{A2} \\ \theta_2 \end{bmatrix} \quad (39)$$

$$\begin{pmatrix} \dot{T}_{A3} \\ \dot{\varphi}_3 \\ \dot{t}_{A2} \\ \dot{\theta}_3 \end{pmatrix} = \begin{pmatrix} 2Q_{11}^3 T_o \\ 0 \\ 2Q_{33}^3 t_2 \\ 0 \end{pmatrix} + \begin{bmatrix} -2Q_{11}^3+F_{11}^3 & F_{12}^3 & F_{13}^3 & F_{14}^3 \\ F_{21}^3 & F_{22}^3 & F_{23}^3 & F_{24}^3 \\ F_{31}^3 & F_{32}^3 & -2Q_{33}^3+F_{33}^3 & F_{34}^3 \\ F_{41}^3 & F_{42}^3 & F_{43}^3 & F_{44}^3 \end{bmatrix} \begin{bmatrix} T_{A3} \\ \varphi_3 \\ t_{A2} \\ \theta_3 \end{bmatrix} \quad (40)$$

From Eqn.(36) and (38), we get

$$\left.\begin{aligned} T_1 &= -\frac{A_1}{A_2} T_o + \frac{1}{A_2} T_{A1} \\ T_2 &= \frac{A_1}{A_2} T_o - \frac{1}{A_2} T_{A1} + 2T_{A2} \\ t_1 &= -t_o + 2t_{A1} \\ t_2 &= t_o - 2t_{A1} + 2t_{A2} \end{aligned}\right\} \quad (41)$$

Combine Eqn.(17) with (41), the global differential equation can be obtained.

$$\begin{pmatrix} \dot{T}_{A1} \\ \dot{T}_{A2} \\ \dot{T}_{A3} \\ \dot{\phi}_1 \\ \dot{\phi}_2 \\ \dot{\phi}_3 \\ \dot{t}_{A1} \\ \dot{t}_{A2} \\ \dot{t}_{A3} \\ \dot{\theta}_1 \\ \dot{\theta}_2 \\ \dot{\theta}_3 \end{pmatrix} = \begin{pmatrix} Q_{11}^1 (1+\frac{A_1}{A_2}) T_o \\ -2Q_{11}^2 \frac{A_1}{A_2} t_o \\ 2Q_{11}^3 \frac{A_1}{A_2} T_o 0 \\ 0 \\ 0 \\ 2Q_{33}^2 t_o \\ -2Q_{33}^3 t_o \\ 2Q_{33}^1 t_o \\ 0 \\ 0 \\ 0 \end{pmatrix} + \begin{bmatrix} -\frac{Q_{11}^1}{A_2}+F_{11}^1 & 0 & 0 & F_{12}^1 & 0 & 0 & 0 & 0 & 0 & F_{14}^1 & 0 & 0 \\ 2\frac{Q_{11}^2}{A_2} & -2Q_{11}^2+F_{11}^2 & 0 & 0 & F_{12}^2 & 0 & 0 & 0 & 0 & 0 & F_{14}^2 & 0 \\ -\frac{2Q_{11}^3}{A_2} & 4Q_{11}^3 & -2Q_{11}^3+F_{11}^3 & 0 & 0 & F_{12}^3 & 0 & 0 & 0 & 0 & 0 & F_{14}^3 \\ F_{21}^1 & 0 & 0 & F_{22}^1 & 0 & 0 & 0 & 0 & F_{23}^1 & 0 & 0 & 0 \\ 0 & F_{21}^2 & 0 & 0 & F_{22}^1 & 0 & F_{23}^2 & 0 & 0 & 0 & 0 & 0 \\ 0 & 0 & F_{21}^3 & 0 & 0 & F_{22}^3 & 0 & F_{23}^3 & 0 & 0 & 0 & 0 \\ 0 & 0 & 0 & 0 & F_{32}^2 & 0 & -2Q_{33}^2+F_{33}^2 & 0 & 0 & 0 & 0 & 0 \\ 0 & 0 & 0 & 0 & 0 & F_{32}^3 & 4Q_{33}^3 & -2Q_{33}^3+F_{33}^3 & 0 & 0 & 0 & 0 \\ 0 & 0 & 0 & F_{32}^1 & 0 & 0 & -4Q_{33}^1 & 4Q_{33}^1 & -2Q_{33}^1+F_{33}^1 & 0 & 0 & 0 \\ F_{41}^1 & 0 & 0 & 0 & 0 & 0 & 0 & 0 & 0 & F_{44}^1 & 0 & 0 \\ 0 & F_{41}^2 & 0 & 0 & 0 & 0 & 0 & 0 & 0 & 0 & F_{44}^2 & 0 \\ 0 & 0 & F_{41}^3 & 0 & 0 & 0 & 0 & 0 & 0 & 0 & 0 & F_{44}^3 \end{bmatrix} \begin{bmatrix} T_{A1} \\ T_{A2} \\ T_{A3} \\ \phi_1 \\ \phi_2 \\ \phi_3 \\ t_{A1} \\ t_{A2} \\ t_{A3} \\ \theta_1 \\ \theta_2 \\ \theta_3 \end{bmatrix} \quad (42)$$

Eqn. (42) can be solved numerically.

The design data for the CAES recuperat is shown in Tables 1 and 2. Figures 7 and give the time functions of inlet and outlet temperature of the flow on each side. Figure 7 shows the plot of results using linear shape functions. The instability occurs only at the initial period of time. Figure 8 shows the results obtained using modified non-linear shape function. It can be seen that the instability problem has been eliminated. The steady state outlet temperatures for the flue gas and air are 300°F and 546.6°F, respectively.

Table 1 Material Properties

	Tube Side Fluid	Tube Metal	Shell Side Fluid	Shell Metal
Heat Capacity, Btu/lb.°F	0.24	0.11	0.26	0.11
Density, lb/ft^3	0.083	490.0	0.083	490.0

Table 2 Geometry and Design Data for the Model

	Unit 1	Unit 2	Unit 3
A_i, ft^2	30314.0	12992.0	25983.0
A_{si}, ft^2	895.2	383.67	743.35
V_{ai}, ft^3	1576.0	675.5	1351.0
V_{ti}, ft^3	614.41	263.3	526.6
V_{fi}, ft^3	2605.0	1116.4	2120.7
V_{si}, ft^3	875.7	375.3	727.2
h_a, Btu/ft^2.min.°F	2.33	2.15	2.23
h_f, Btu/ft^2.min.°F	0.133	0.12	0.115
h_s, Btu/ft^2.min.°F	0.036	0.036	0.036

CONCLUSION

A systematic method has been presented to estimate transient response of cross-flow shell-and-tube heat exchangers with large thermal inertia. The approach has been developed in a way that numerical tools can be easily applied. Though assumptions have been made to simplify the formulation, our case study indicates that the accuracy is adequate for industry performance prediction.

REFERENCE

[1] Singh, K.P., Soler, A.I., Mechanical Designs of Heat Exchangers and Pressure Vessel Components, Arcturus Publishers Inc., 1984.

[2] Shin, T.M., Numerical Heat Transfer, Hemisphere Publishing Comp., 1984.

[3] Runchal, A.K., Convergence and Accuracy of Three Finite Difference Schemes for a Two-dimensional Conduction and Convection Problem, Int. J. Numer. Methods Eng., vol. 4, pp541-550, 1972

[4] Raithby, G.D.,Torrance, K.E., Upstream-weighted Difference Schemes and Their Application to Elliptic Problems Involving Fluid Flow, Comput. Fluids, Vol. 2,pp.191-206,1974

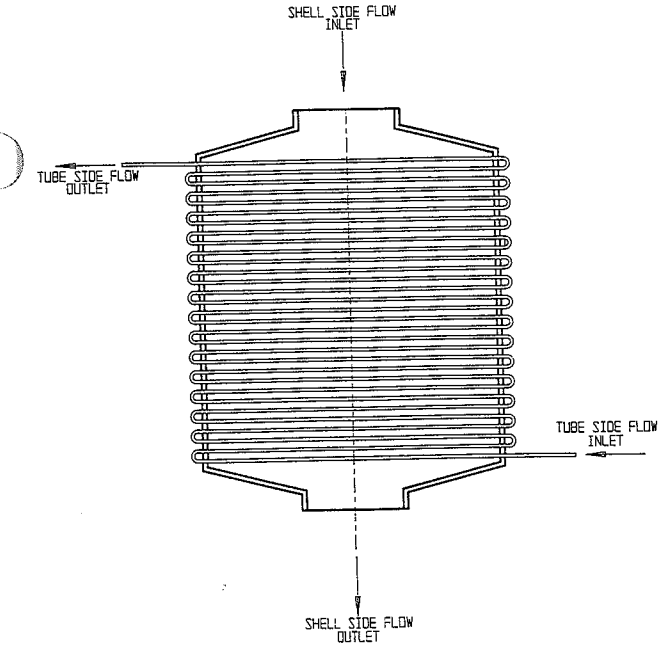

FIGURE 1 TYPICAL CROSS FLOW SHELL-AND-TUBE HEAT EXCHANGER

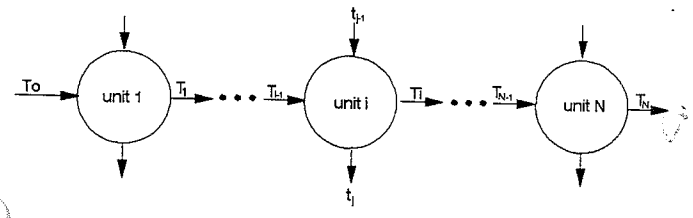

Figure 2 Heat Transfer Unit Mesh for Cross Flow Shell-and-Tube Heat Exchangers

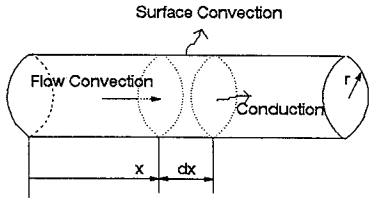

Figure 3 Conservation of Energy Over a Small Control Volume Disk

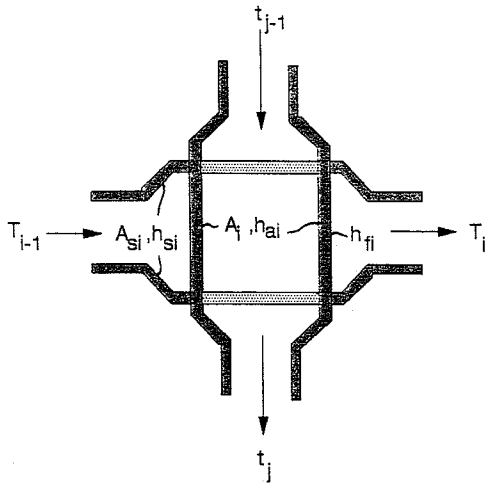

Figure 4 A Cross Flow Heat Transfer Unit

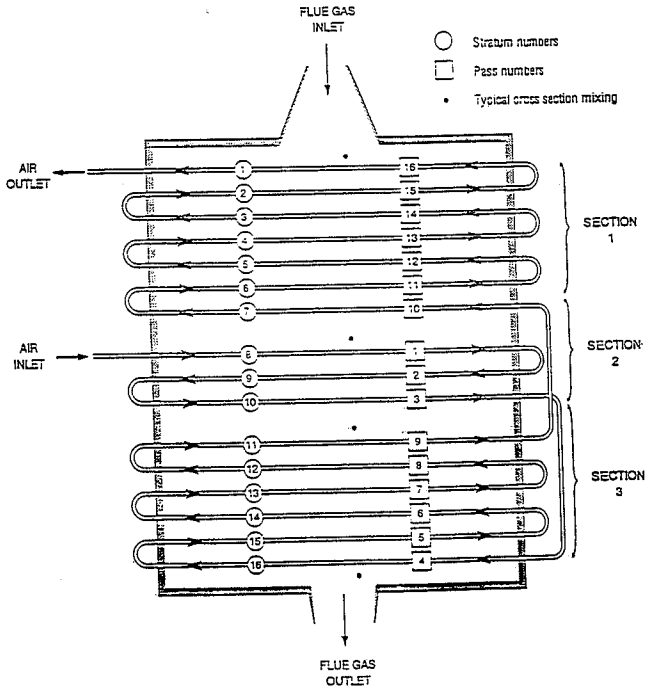

Figure 5 A Preheating Recuperator in CAES Plant

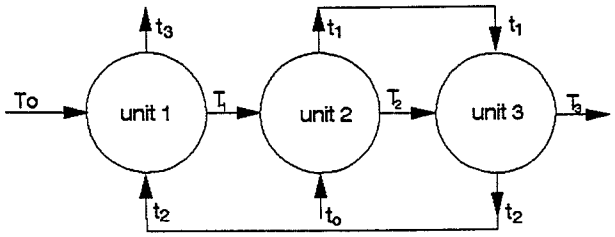

Figure 6 Heat Transfer Unit Mesh for the Recuperator

Figure 7 Results Using Linear Shape Functions

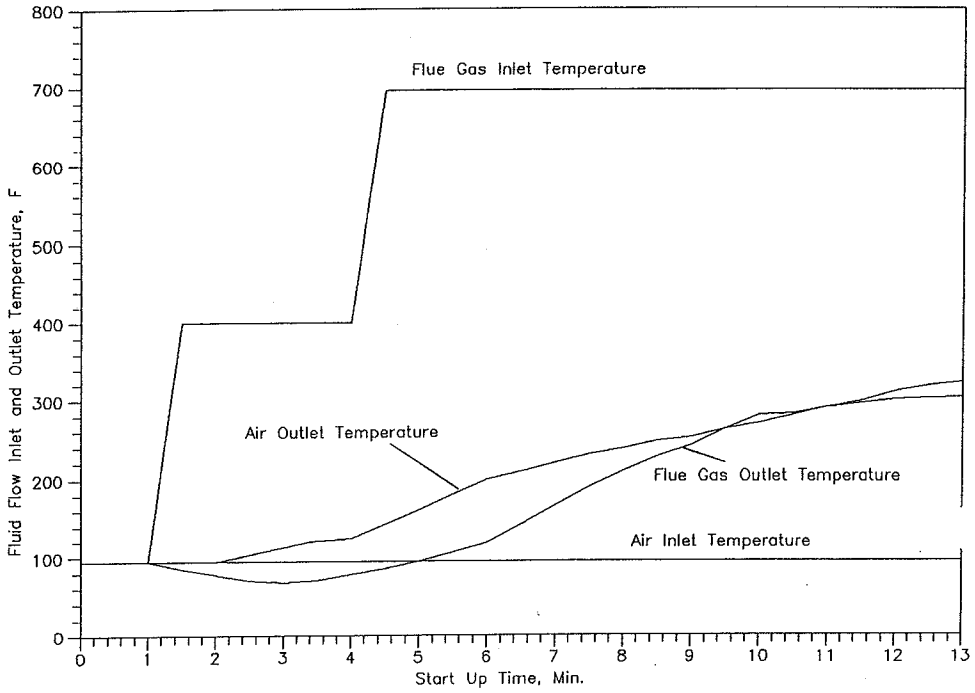

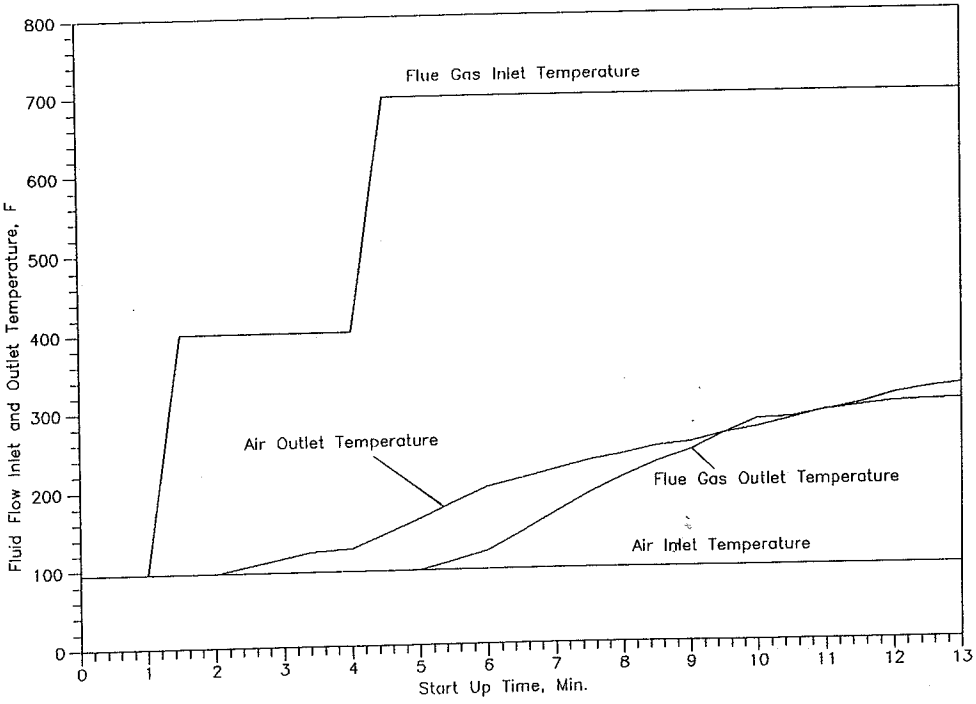

Figure 8 Results Using Non-Linear Shape Functions